Materials Letters 173 (2016) 127–130

Contents lists available at ScienceDirect

Materials Letters

journal homepage: www.elsevier.com/locate/matlet

Evanescent field optimization on Y-branch silicon nitride optical waveguide for biosensing

A.H. Reshak [a,c,*], M.M. Shahimin [b], K.N. Khor [a,b,c], M.H.A. Wahid [b], N.A.M Ahmad Hambali [b]

[a] New Technologies – Research Centre, University of West Bohemia, Univerzitni 8, 306 14 Pilsen, Czech Republic
[b] Semiconductor Photonics and Integrated Lightwave System (SPILS), Tun Abdul Razak Laser Lab Laboratory (TAReL) School of Microelectronic Engineering, Universiti Malaysia Perlis (UniMAP), Pauh Putra Main Campus, Jalan Arau, Changlun, 02600 Arau, Perlis, Malaysia
[c] Center of Excellence Geopolymer and Green Technology, School of Material Engineering, University Malaysia Perlis, 01007 Kangar, Perlis, Malaysia

ARTICLE INFO

Article history:
Received 28 November 2015
Accepted 27 February 2016
Available online 2 March 2016

Keywords:
Integrated optic
Y-branch splitter
Beam propagation method
Evanescent field optimization

ABSTRACT

Evanescent field had been widely used in bio and chemical sensors. However in most cases, evanescent field is not maximized and consequently produced an unoptimized sensor performance. It is the aim of the paper to optimize the design of 1:2 Y-branch splitter optical waveguide through simulation by using FD-BPM. Y-branch splitter are simulated to optimize the power loss. Width of waveguide and effective angle are manipulated in the power loss optimization. The result shows that evanescent field is maximized at optimized thickness and width. The result suggests that Y-branch splitter with width of 25 μm and effective angle of 6.24° is the best design for evanescent field sensor application with both high sensitivity and signal to noise ratio.

1. Introduction

Waveguide based bio and chemical sensors, utilizing evanescent field have attracted a lot of attention in the past decade due to its versatility and advantages. Some of the major advantages are its simplicity, robustness and label-free measurement [1]. A lot of research has been conducted on waveguide configurations namely, linear and Y-branch for creating integrated optics for various applications. However, in the literature so far, there are only optimization of linear waveguides; both in simulation and experimental for various applications including biosensors [2–4]. Although usage of Y-branch in integrated optics sensors has been implemented [5,6], direct optimization of Y-branch optical waveguide had been limited to only in optical communications [7–9].

Therefore, in this work we proposed a direct optimization of Y-branch to be used for biosensor application via enhanced evanescent field penetration and minimal power loss. Finite difference beam propagation method (FD-BPM) is used in this paper to provide 3D optical waveguide structure with high non-linearity such as bending and tapering [10]. Y-branch splitter is used in this context as evanescent field sensor with one of the output branch served as sensing site and the other as reference [11]. Hence, the difference between output power can be detected directly and instantly which is advantageous compared to linear waveguide that is used in Ref. [12-14].

2. Methodology

Fig. 1(a) illustrated the scattering of evanescent excitation binding of analyte on the waveguide surface. Y-branch splitter, as illustrated in Fig. 1(b), is simulated and designed with the aim of minimizing power loss. TE polarization with wavelength of 1.064 μm is used in Y-branch simulation with thickness and width of 0.1 μm and 4 μm respectively. Refractive index of cladding, waveguide and substrate layer is 1.33, 1.98 and 1.45 which correspond to water, silicon nitride and silicon oxide respectively.

$$\theta_{eff} = 2 \times \tan^{-1}\frac{(X_{off}/2)}{L_{off}} \quad (1)$$

Y-branch splitter is constructed in the simulation software by using bending waveguide structure with input waveguide width to be twice the size of branch waveguide. X_{off}, L_{off} and θ_{eff} are the parameters that characterize Y-branch splitter (see Fig. 1(c)). X_{off} is the distance between two output branches, L_{off} is the horizontal distance of bending waveguide and θ_{eff} is effective angle of Y-branch splitter which is related to X_{off} and L_{off} as shown in Eq. (1).

Simulation of Y-branch splitter with variation of start location of bending waveguide for mode conversion loss enhancement is known as location optimization. Start location is varied from 205 μm to 155 μm with step of 5 μm in simulation of location

* Corresponding author at: New Technologies – Research Centre, University of West Bohemia, Univerzitni 8, 306 14 Pilsen, Czech Republic.
E-mail address: maalidph@yahoo.co.uk (A.H. Reshak).

http://dx.doi.org/10.1016/j.matlet.2016.02.142
0167-577X/

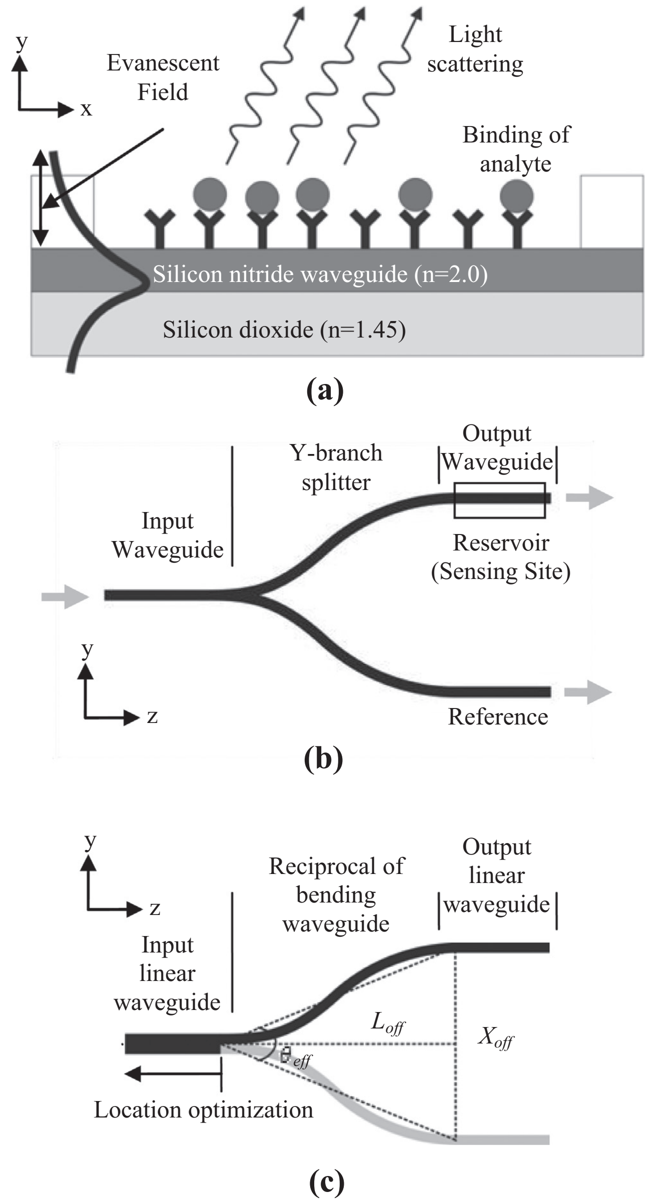

Fig. 1. (a) Scattering of evanescent excitation binding of analyte on the waveguide surface; (b) Y-branch splitter used as evanescent field biosensor; (c) Model of Y-branch splitter without taper.

optimization. The range of L_{off} used in investigation of Y-branch splitter are from 300 to 2100 μm with step of 200 μm and result in θ_{eff} that is in the range of approximately 3–22°. As the L_{off} increases, θ_{eff} and slope of bending waveguide reduces while length of bending waveguide increases. Simulation is repeated to perform location optimization to maximize the power output (*Pout*) at each effective angle. The simulation is followed by the increment of the width of Y-branch splitter from 4 μm to 10 μm with location optimization. This is due to the fact that more power can be confined in the waveguide and thus theoretically, it can reduced the bending loss of the waveguide structure. Width of the waveguide is further increased to 15 μm, 20 μm and 25 μm without location optimization so that relation of width to output power can be further investigated.

3. Results and discussion

Fig. 2(a) shows the result of *Pout* as a function of effective angle for Y-branch splitter with input width of 8 μm and branching width is 4 μm. It can be seen that location optimization increases *Pout* significantly, especially at smaller θ_{eff}. *Pout* profile of Y-branch splitter increased gradually as effective angle is increased to a peak at 13.68° followed by a rapid decrement with larger angles. *Pout* profile is mainly affected by the bending loss which is in turn affected by the effective angles. Gradual increment of *Pout* is caused by the optimized effective angle which resulted in optimized branching angle and length of bending waveguide. In return, rapid decrement of the *Pout* is caused by shorter length of the bending waveguide with rapid increment of rate of the bending loss.

Fig. 2(b) shows the result of *Pout* as function of the effective angle for input width of 20 μm with and without location optimization. It can be seen that increment of *Pout* caused by location optimization is insignificant for width of 10 μm (or input width of 20 μm). This is due mainly to the increasing number of mode as width increases and thus the mode beating profile changes in input waveguide as shown in Figs. 3(a) and (b). Due to this reason, location optimization is not performed in Y-branch splitter with bigger input width than 20 μm.

Fig. 3(c) shows the *Pout* as function of effective angle for input width of 8 μm, 20 μm, 40 μm and 50 μm. It can be seen that the increment of *Pout* for input of 20 μm from 8 μm is significant whereby *Pout* is increased by 19.7%. The increment is mainly due to the better power confinement in the bending waveguide and thus the bending loss is reduced regardless of effective angle. However, increment of *Pout* become smaller as input width is

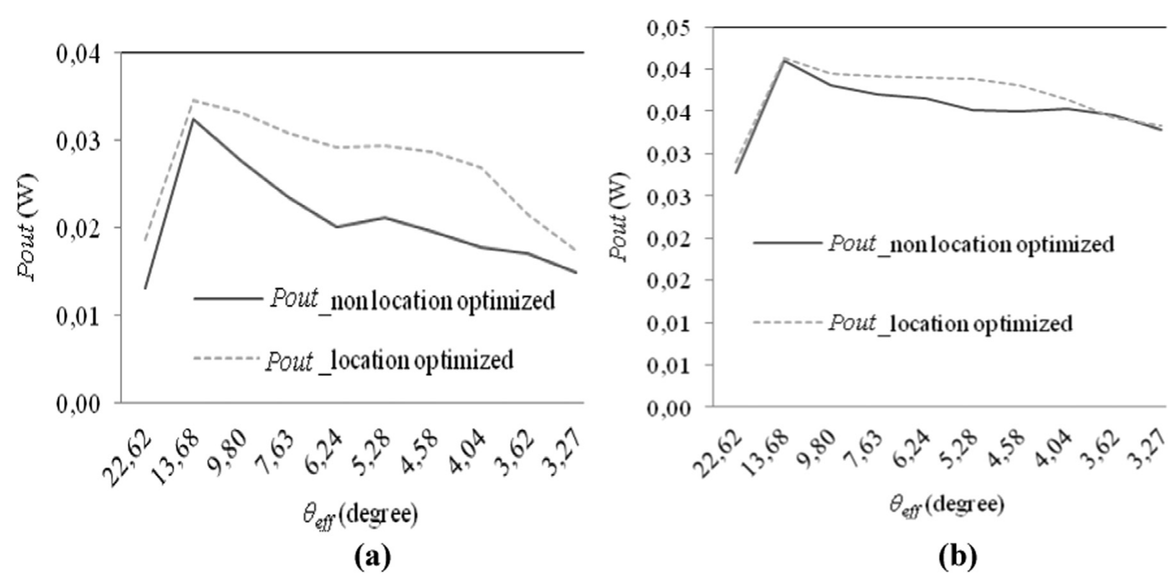

Fig. 2. (a) *Pout* as function of effective angle with and without location optimization for input width of 8 μm; (b) *Pout* as function of effective angle with and without location optimization for input width of 20 μm.

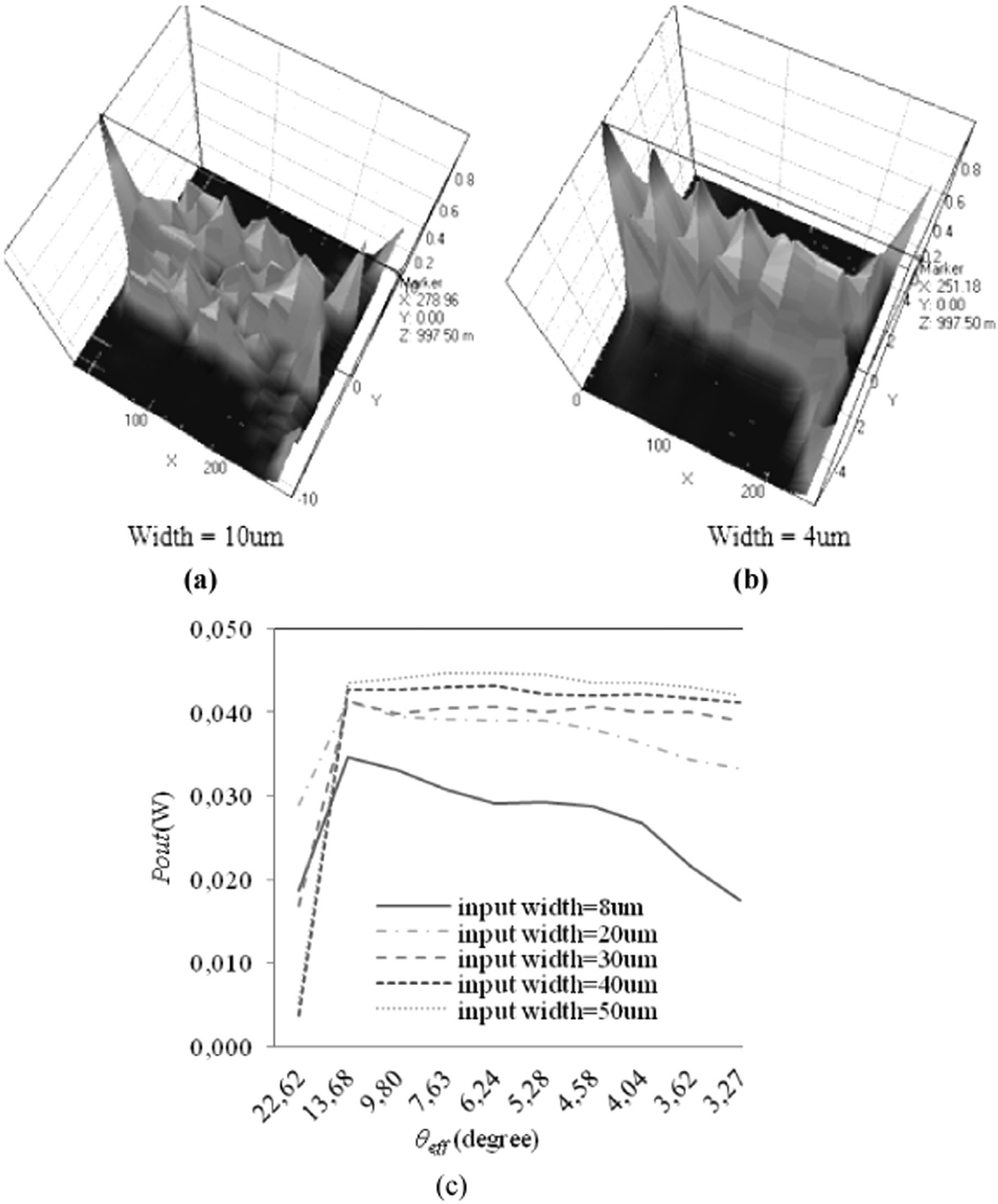

Fig. 3. (a) Mode beating profile of input waveguide for width of 10 μm; (b) 4 μm respectively; (c) *Pout* as function of effective angle for input width of 8 μm, 20 μm, 30 μm, 40 μm and 50 μm. Location optimization is performed only on Y-branch with input width of 8 μm and 20 μm.

further increased to 30 μm, 40 μm and 50 μm. *Pout* increment is caused by reducing bending loss and increased power transmission at coupling of laser source. On the other hand, *Pout* increment is limited by maximum power transmitted from input waveguide into bending waveguide since power in input waveguide is increased by 1.33% only with width of waveguide doubled. As a result, *Pout* is almost saturated by optimization of bending loss after the input width is increased to 20 μm and further increment of width increases *Pout* by slight increment of power in input waveguide. At input width of 50 μm, the maximum *Pout* is 0.045 W.

4. Conclusion

Y-branch splitter with optimized evanescent field and minimum power loss has been designed to improve sensitivity and signal to noise ratio of the biosensor. The output power was found to reach its maximum at effective angle of 13.68°. For larger angles, the Y-branch splitter suffered severe bending loss. However, it had also been found that the output power was reduced further with smaller width. This decrement is mainly due to the longer length of bending waveguide that suffers bending loss. Bigger widths of bending waveguide showed better power confinement and subsequently reduced the bending loss. The results showed that Y-branch splitter required the waveguide width of 25 μm in order to reach the optimum power of 0.045 W. Results in this paper suggested that Y-branch splitter of 25 μm width, effective angle of 6.24° and thickness of 0.1 μm to be the direct optimum design for evanescent field sensor application with both high sensitivity and signal to noise ratio.

Acknowledgment

The authors would like to thank Dr Steve Dods for helpful advices and fruitful discussions. ERGS (9010-00004) and RACE (9017-00002) from Ministry of Higher Education are acknowledged for the funding used for this investigation. A.H. Reshak would like to acknowledge the CENTEM project, reg. no. CZ.1.05/2.1.00/03.0088, cofunded by the ERDF as part of the Ministry of Education, Youth and Sports OP RDI Programme and, in the follow-up sustainability stage, supported through CENTEM PLUS (LO1402) by financial means from the Ministry of Education, Youth and Sports under the National Sustainability Programme I. Also would like to acknowledge MetaCentrum (LM2010005) and CERIT-SC (CZ.1.05/3.2.00/08.0144) infrastructures.

References

[1] X. Fan, et al., Sensitive optical biosensors for unlabeled targets: a review, Anal. Chim. Acta 620 (2008) 8–26.
[2] K. K. Nan and M. M. Shahimin, Optimisation of ion-exchanged channel waveguides for optical manipulation, in: Proceedings of the IEEE Regional Symposium on Micro and Nano Electronics, Kota Kinabalu, Sabah, 2011, pp. 383–387.
[3] M. M. Shahimin, et al., Optical propulsion of mammalian eukaryotic cells on an integrated channel waveguide, in: Proceedings of the Microfluidics, BioMEMS, and Medical Microsystems IX, San Francisco, CA, 2011.
[4] K. N. Khor, et al., Copper ion-exchanged channel waveguides optimization for optical trapping, Progress in Biophysics and Molecular Biology.
[5] P. Hua, et al., Integrated optical fluorescence multisensor for water pollution, Opt. Express 13 (2005) 1124–1130.
[6] P. Hua, et al., Integrated optical dual Mach-Zehnder interferometer sensor, Sens. Actuators B: Chem. 87 (2002) 250–257.
[7] L.W. Xie, et al., Optical waveguide electric field sensor with controllable operating point using asymmetric Mach-Zehnder structure, Optoelectron. Lett. 9 (2013) 81–84.
[8] R. Singhal, et al., Fabrication of single-mode Y-branch waveguides in photosensitive polymer with reduced Y-junction residue, Optik 123 (2012) 1911–1914.
[9] P. Rani, et al., Realization of and gate in y shaped photonic crystal waveguide, Opt. Commun. 298-299 (2013) 227–231.
[10] K. Kawano, T. Kitoh (eds.), Introduction to optical waveguide, in: Analysis: Solving Maxwell's Equations and the Schrodinger Equation, John Wiley & Sons Canada, 2001.
[11] G. Pandraud, et al., Evanescent wave sensing: new features for detection in small volumes, Sens. Actuators A: Phys. 85 (2000) 158–162.
[12] M.D. Stephens, et al., Optical and physical characterization of a local evanescent array coupled biosensor: use of evanescent field perturbations for multianalyte sensing, Sens. Actuators B: Chem. 145 (2010) 769–774.
[13] H. Chih-Wei, et al., Compact Y-branch power splitter based on simplified coherent coupling, Photonics Technol. Lett. IEEE 15 (2003) 1103–1105.
[14] W. Qian, et al., A low-loss Y-branch with a multimode waveguide transition section, Photonics Technol. Lett. IEEE 14 (2002) 1124–1126.